



Identification of Groundwater Aquifers Using Geoelectric Methods with Schlumberger Configuration in Peatland Areas, West Kalimantan, Indonesia

RasmiDepartement of Physics,
Universitas Tanjungpura,
INDONESIA**Yuris Sutanto***Departement of Physics,
Universitas Tanjungpura,
INDONESIA**Radhitya Perdhana**Departement of Geophysics,
Universitas Tanjungpura,
INDONESIA**Muliadi**Departement of Geophysics,
Universitas Tanjungpura,
INDONESIA**Muhardi**Departement of Geophysics,
Universitas Tanjungpura,
INDONESIA**Mahmuddin Marbun**Department of Mechanical Engineering,
Universitas Teuku Umar,
INDONESIA**Amir Machmud**Graduate Institute of Environmental
Engineering, National Central University,
TAIWAN**Elok Surya Pratiwi**Department of Geography,
National Taiwan Normal University,
TAIWAN***Correspondence: E-mail:** yuris@physics.untan.ac.id

Article Info**Article history:**

Received: December 20, 2023

Revised: January 25, 2024

Accepted: April 09, 2024



Copyright : © 2024 Foundae (Foundation of Advanced Education). Submitted for possible open access publication under the terms and conditions of the Creative Commons Attribution - ShareAlike 4.0 International License (CC BY SA) license (<https://creativecommons.org/licenses/by-sa/4.0/>).

Abstract

The geoelectric-resistivity method with Schlumberger configuration is commonly used for groundwater exploration. This method helps identify changes in the resistivity of rock layers beneath the Earth's surface by flowing direct current (DC). In this research, geoelectric-resistivity was used to search for the existence of groundwater aquifers in water crisis areas with peat soil structures. In addition, this research aims to determine the depth of the aquifer layer based on resistivity values below the surface and to identify variations in resistivity values below the surface. The method used in this research was the Schlumberger configuration resistivity geoelectric method with 4 measurement points, each with a stretch length of 500 m. The research results show that the subsurface resistivity value in the Parit Haji Muksin II area is 2.69 Ωm to 264 Ωm. The unconfined aquifer at the research location was found at point 1 and point 2 at a depth of 3.94 m to 35.5 m, while the confined aquifer was found at points 3 and 4 at a depth of 13.6 m to 61.8 m. This study indicates the presence of potential groundwater resources in tropical peatlands, highlighting the necessity for further comprehensive research to ensure their sustainable utilization in the future

Keywords: geoelectric; groundwater aquifers; peatland areas; resistivity; schlumberger

To cite this article: Rasmi, R., Yuris. S., Perdhana, R., Muliadi, M., Muhardi, M., Sadjab, B. A., Marbun, M. and Pratiwi, E. S. (2024). Identification of Groundwater Aquifers Using Geoelectric Methods with Schlumberger Configuration in Peatland Areas, West Kalimantan, Indonesia. *International Journal of Hydrological and Environmental for Sustainability*, 3(1), 08-17. <https://doi.org/10.58524/ijhes.v3i1.388>

INTRODUCTION

Parit Baru Village, Sungai Raya District, Kubu Raya Regency, has a population of 31,149 people, compared to the population in 2017, which had a population of 29,668 people. This shows the population increased by 14.81% over the five years from 2017 to 2023. An increase in population

will cause an increase in the need for facilities and infrastructure, one of which is the need for clean water (Sabara et al., 2022). Parit Baru Village is one of the villages in Sungai Raya District whose clean water needs still come from rainwater, shallow wells, and drilled wells. One of the areas in Parit Baru Village, namely Parit Haji Muksin II, has extensive peatlands, which can affect water quality. The use of rainwater and shallow wells is considered less efficient because shallow wells are easily polluted during the rainy season and turbidity easily occurs during the dry season. Efforts to fulfill clean water needs are also carried out by the government through PDAM (Anggereni & Ikbal, 2018; Bott et al., 2021; Handayani & Puspasari, 2020; Sudirman et al., 2018). However, there are still several locations that do not have these facilities, including the research location where the Baitul Ibadah College will be built on Jalan Parit Haji Muksin II. Therefore the availability of groundwater is crucial in area lacking access to PDAM services, such as the research location. According to observations at the research location, well data shows the depth of shallow wells is more than 5 meters and that of drilled wells is more than 40 meters (Al-ahmadi & El-Fiky, 2009; Brindha & Elango, 2012). Making shallow wells is traditionally done by digging the ground to the spring point below the surface, while drilling wells is conducted using more sophisticated tools to predict the depth of the groundwater aquifer layer. Groundwater that moves and collects between soil particles seeps into the soil and forms a layer called an aquifer (Tsunomori et al., 2017; You et al., 1996).

Aquifers consist of rocks such as sand and gravel, which have high porosity and permeability, enabling them to store and release significant amounts of water (Fatchurohman et al., 2018). Groundwater within the aquifer system, also referred to as the groundwater aquifer, plays a vital role in fulfilling the clean water requirements of the community. One method that can be used to identify groundwater aquifers is the geoelectric method (Fatchurohman et al., 2018). To date, the use of the Vertical Electrical Sounding (VES) method in groundwater aquifer exploration has been widely used by previous researchers (Aizebeokhai & Oyeyemi, 2015; Prabowo et al., 2022). The VES method has various types of configurations, one of which is the Schlumberger configuration. The purpose of this configuration is to study vertical variations in the resistivity of rocks below the surface (sounding) so that it can be used to identify deeper objects, such as aquifer layers (Abidin et al., 2011; Pratiwi et al., 2019). Therefore, this research was carried out to identify groundwater aquifers using the Schlumberger configuration geoelectric resistivity method in Parit Baru Village, Sungai Raya District, Kubu Raya Regency.

Peatlands

Peatlands are terrestrial wetland ecosystems in which waterlogged conditions prevent plant material from fully decomposing. Consequently, the production of organic matter exceeds its decomposition, resulting in a net accumulation of peat. These unique ecosystems occur in various climatic zones and continents, covering approximately 4 million square kilometers globally. To put that in perspective, peatlands constitute about 70% of natural freshwater wetlands or approximately 3% of the Earth's land surface (Négrel et al., 2010; Zoysa et al., 2021).

Peatlands serve as carbon-rich ecosystems, storing and sequestering more carbon than any other type of terrestrial ecosystem. Unfortunately, when peatlands are drained, the carbon from the organic matter in peat dries up and gradually oxidizes into CO₂, leading to permanent loss from the system. Therefore, proper water table management is essential for restoring hydrology and preventing soil compaction and subsidence caused by drained peatlands (Custodio, 2015; FAO, 2016; Gordon et al., 2008).

These fascinating ecosystems occur in different regions: 1). Northern and temperate peatlands: The majority of the world's peatlands are found in boreal and temperate parts of the Northern Hemisphere, including Europe, North America, and Russia. These regions have formed under high precipitation-low temperature climatic conditions. 2). Tropical peatlands: In the humid tropics, peat can form under high precipitation and high temperature conditions. Southeast Asia, mainland East Asia, the Caribbean, Central America, South America, Africa, parts of Australasia, and a few Pacific Islands host tropical peatlands. Most of these are located at low altitudes, where rainforest vegetation grows on a thick layer of organic matter. Some tropical peatlands even exist under mangrove forests (Meijaard et al., 2019; Team, 2016; Zoysa et al., 2021). In temperate climates, peatland vegetation primarily consists of Sphagnum mosses, sedges, and shrubs, which are the primary contributors to peat formation. In tropical climates, graminoids (grasses and grass-like plants) and woody vegetation

play a significant role in providing organic matter for peat accumulation (Li et al., 2018; Meijaard et al., 2019; Poitrasson et al., 1999).

METHOD

This research was carried out on Jalan Parit Haji Muksin II, in Parit Baru Village, Sungai Raya District, Kubu Raya Regency, West Kalimantan (Figure 1). Data acquisition was carried out at 4 measurement points, with sounding point 1 located at coordinates $0^{\circ}06'58, 15''S$ and $109^{\circ}21'44.34''E$, sounding point 2 at coordinates $0^{\circ}07'00.94''S$ and $109^{\circ}21'42.80''E$, sounding point 3 at coordinates $0^{\circ}07'03.93''S$ and $109^{\circ}21'41.38''E$, and sounding point 4 at coordinates $0^{\circ}07'09.66''S$ and $109^{\circ}21'41.09''E$.

This study used 4 electrodes consisting of 2 current electrodes and 2 potential electrodes, the electrodes were arranged in a straight line with the current electrode distance being greater than the potential electrode distance (Nomura et al., 2004; Savira & Suharsono, 2013). The data obtained from direct measurements in the field was in the form of data on electric current strength (I) and potential difference (V) from each measurement point, then data processing was carried out using IP2Win software to obtain the actual resistivity value and obtain a 1D model.

The data collection used four electrodes arranged as in Figure 2. X_{AB} is the distance between the current electrode AB and X_{MN} is the distance between the potential electrode MN. In this study, the smallest X_{MN} distance was 0.3 m, then shifting was carried out 3 times to 50 m, while the smallest X_{AB} current electrode distance was 1 m to a distance of 500. In the geoelectric method, measurements begin by injecting current into the earth by the electrode. current AB. Then, this current will produce a potential difference response and will be measured by the MN potential electrode (Kamiya & Hosono, 2010).

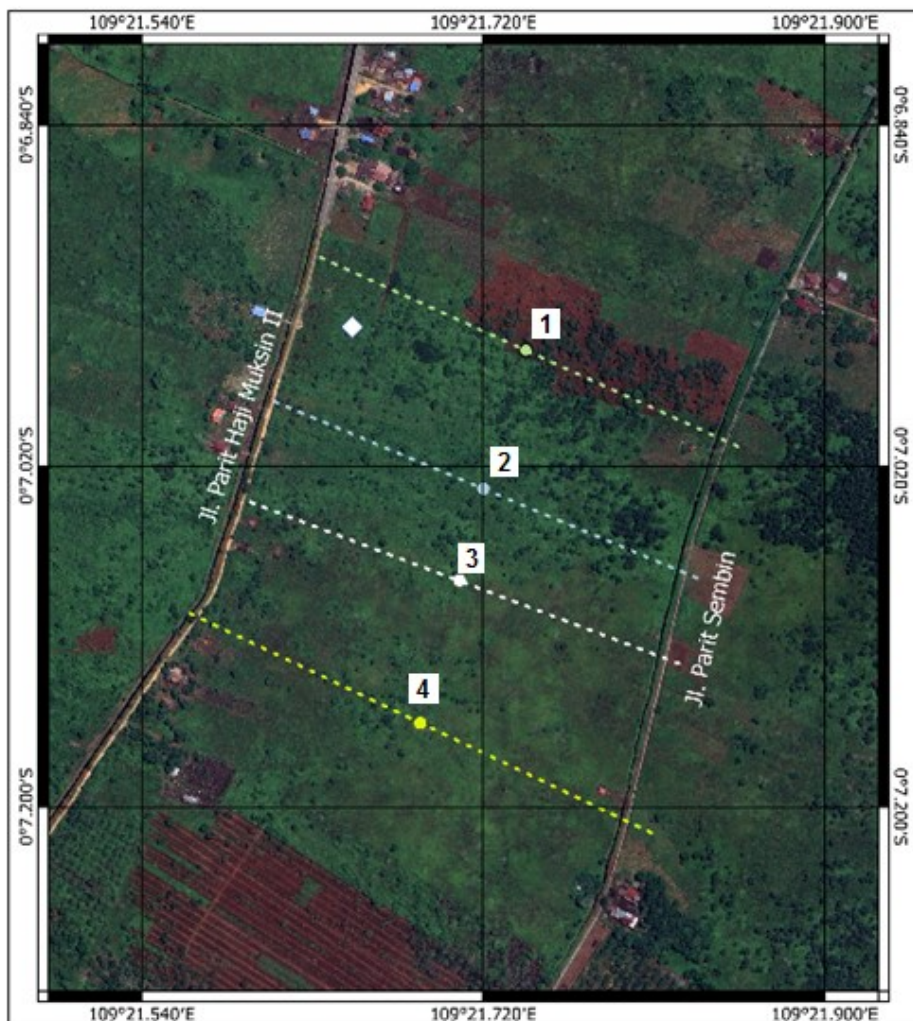


Figure 1. Map of research location and position of sounding points

Data analysis

Data processing will produce resistivity, depth, thickness and curve matching values. The resistivity value obtained from processing is used as a reference for identifying the aquifer layer, by referring to the resistivity value of the earth material as in **Table 1**.

Table 1. Resistivity values of earth materials

Material	Resistivity (Ωm)
Groundwater	0 - 300
Salt water	0,2
Sandstone	1 - 7,4 x 10 ⁸
Clay stone	10 - 10 ⁸
Granite	200 - 10 ⁵
Gravel	100 - 600
Sand	1 - 1.000
Peat	57 - 288

Sources : Data from [\(Sadjab et al., 2020; Saparun et al., 2022\)](#)

In the Schlumberger configuration electrode arrangement, the potential electrode is placed at a fixed distance and is not more than 1/3 the distance of the current electrode. If the measured voltage between M and N drops to a very low value (resulting from the potential gradient decreasing with increasing current electrode distance), a wider distance is given to the potential electrode ([Pratiwi et al., 2019](#)). In the VES method, the distance between the electrodes used is proportional to the rock layer which can be obtained deeper in relation to the distance of the current electrode span ([Satriani et al., 2012](#)). This rock layer that can be detected has a depth (Z) equal to the distance AB/2, as shown in **Figure 2**.

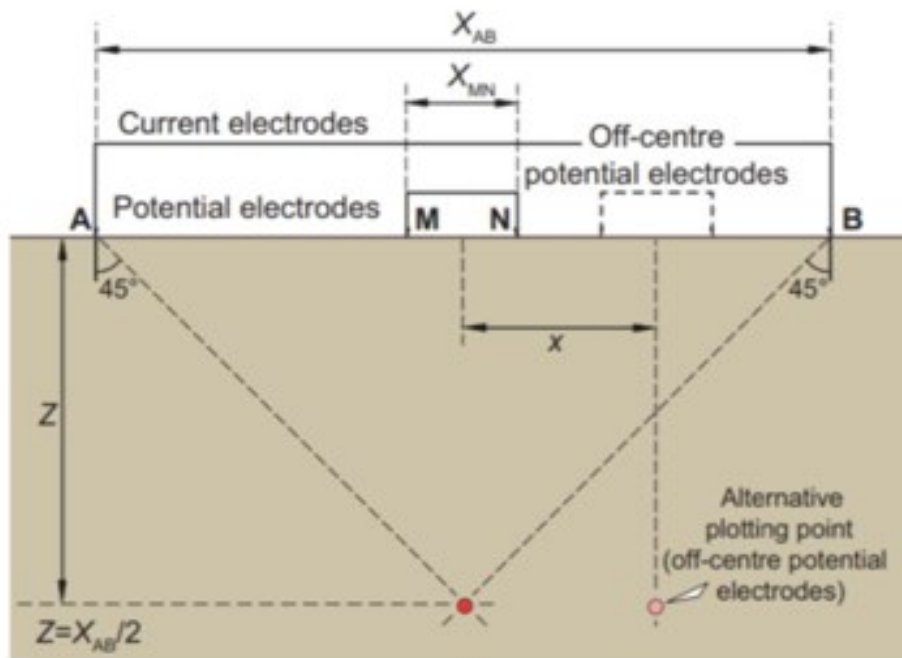


Figure 2. Illustration of VES depth targets

RESULTS AND DISCUSSION

The processing results of the VES data using IPI2win software are in the form of a curve with the black curve and the points representing the apparent resistivity value curve from the observation data. The red curve shows the modeling curve, while the blue curve represents the number and depth

of layers. The results obtained are in the form of an apparent resistivity curve (ρ_a) to depth $AB/2$ and a table of interpretation results of the actual resistivity values at each depth.

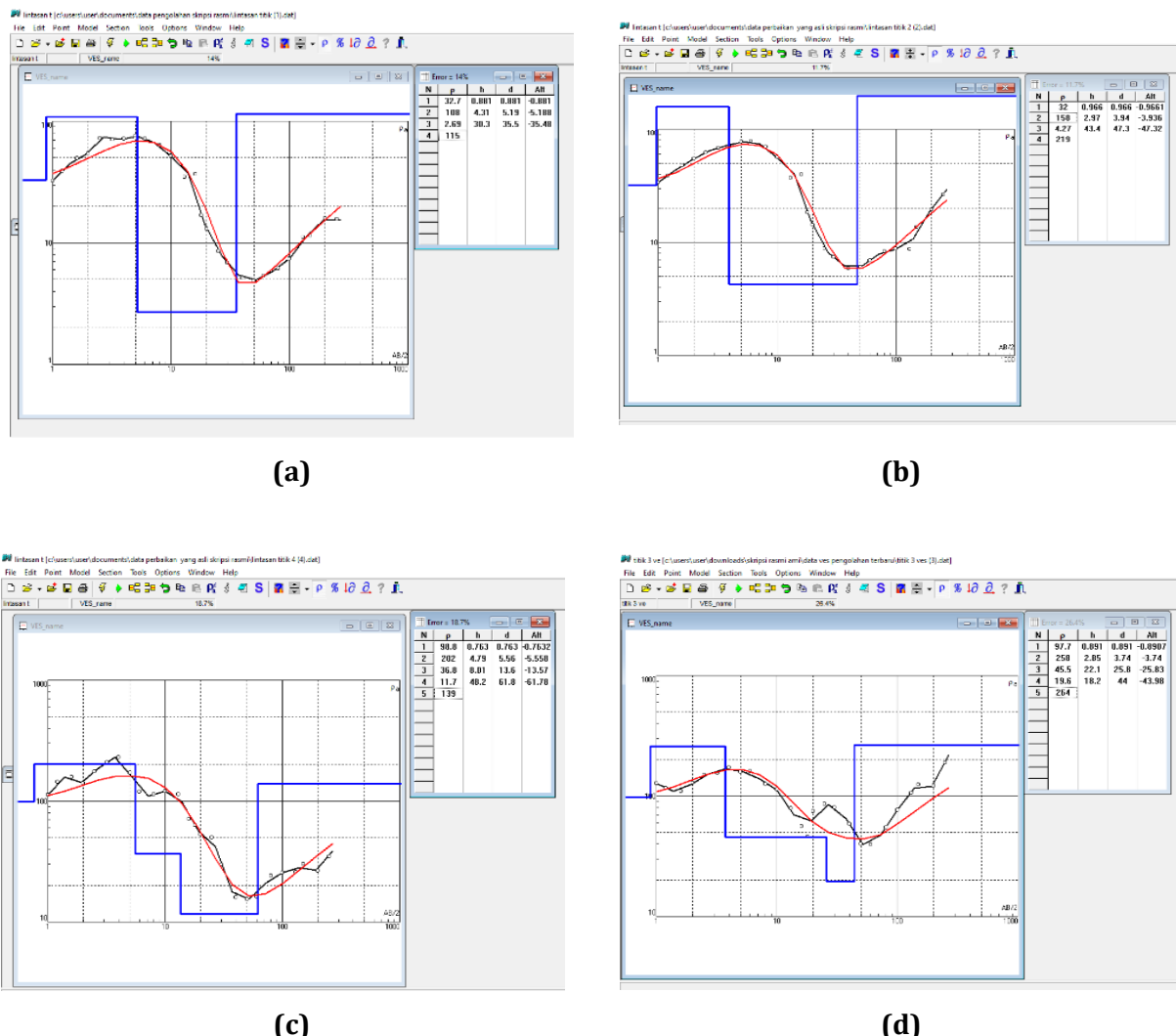


Figure 3. Curve and table of resistivity against depth; (a) sounding point 1, (b) sounding point 2, (c) sounding point 3, and (d) sounding point 4.

Data interpretation is carried out to determine the subsurface layer at each point at the research location by observing the sounding resistivity values resulting from the data processing process (**Figure 3**). This interpretation refers to the rock resistivity table, geological conditions of the research area, and previous research in the surrounding area.

Figures 4, 5, 6, and 7 show the interpretation of subsurface lithology at each sounding point. Based on the interpretation results at each sounding point, 4 to 5 layers were obtained up to a depth of 250 m with lithology in the form of top soil, peat, clay, sand and bedrock.

Based on the measurement results of sounding point 1 as in **Figure 4**, the aquifer layer at point 1 is in the sand layer (third layer). in this case, the sand layer is interpreted as an unconfined aquifer because its depth is still relatively shallow, having a depth of 5.19 m to 35.5 m. The determination of the unconfined aquifer layer is based on its existence conditions, specifically that it has a single impermeable boundary at the bottom, which is the bedrock in the fourth layer. . The identification of the existence of this aquifer layer is supported by data from residents' wells at the research location showing that there are shallow wells at a depth of ± 5 m and drilled wells at a depth of ± 40 m.

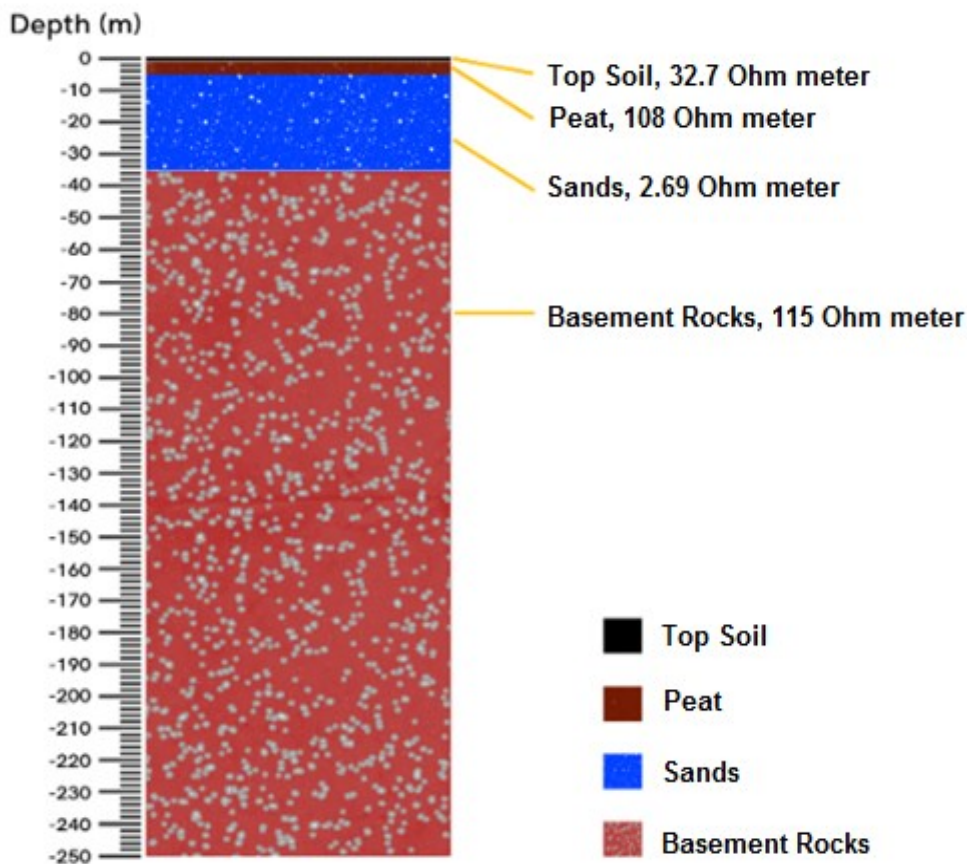


Figure 4. Lithology at sounding point 1

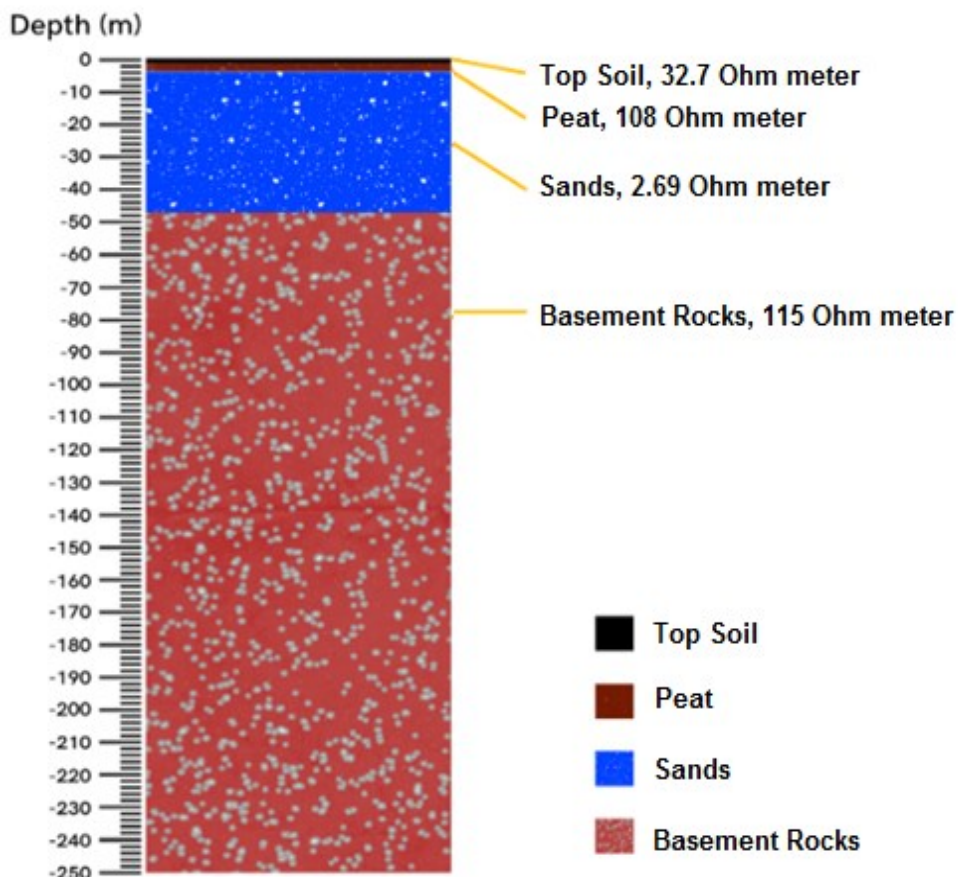


Figure 5. Lithology at sounding point 2

Based on the measurement results of sounding point 2 (**Figure 5**), the aquifer layer at point 1 is in the sand layer (third layer). The third layer is interpreted as an unconfined aquifer because its depth is still relatively shallow, having a depth of 3.94 m – 47.3 m. The determination of the unconfined aquifer layer is also based on the conditions for its existence, namely that it only has one impermeable boundary layer located at the bottom, namely the layer. The fourth is an impermeable layer. The identification of the existence of this aquifer layer is supported by data from residents' wells at the research location showing that there are shallow wells at a depth of \pm 5 m and drilled wells at a depth of \pm 40 m.

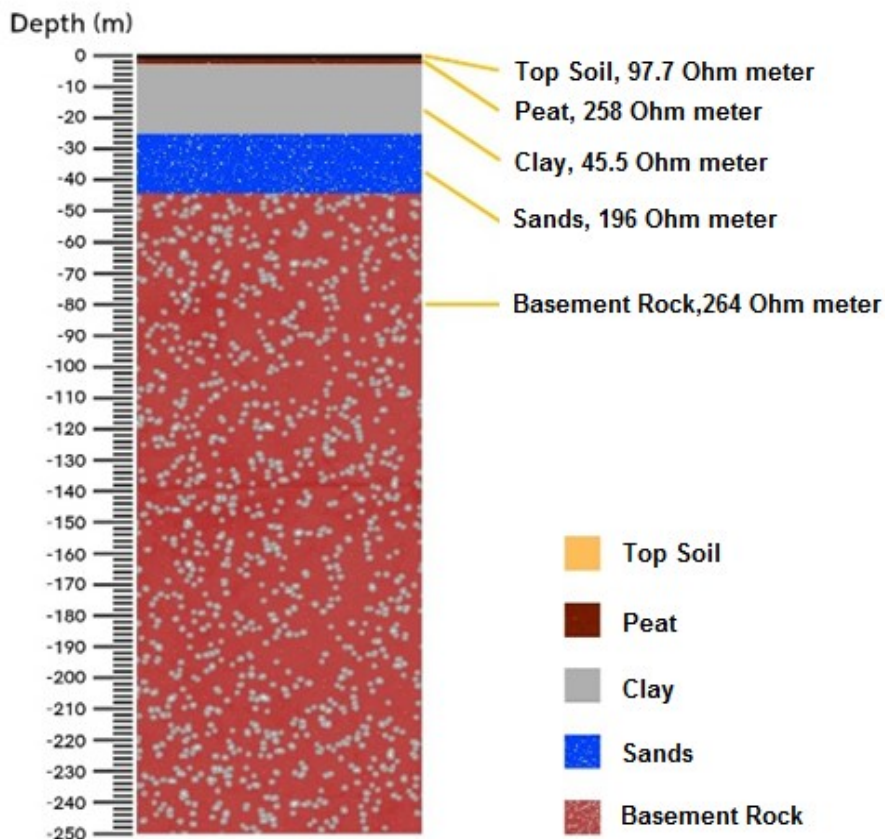


Figure 6. Lithology at sounding point 3

Based on the measurement results of sounding point 3 (**Figure 6**), the aquifer layer at point 3 is in the sand layer (fourth layer) interpreted as a confined aquifer at a depth of 25.8 m – 44 m. It is classified as a confined aquifer because it is situated at a considerable depth and is capped by a clay layer that acts as an aquiclude. The determination of a confined aquifer layer is also based on its position between two impermeable layers. In this case, the sand layer, identified as a confined aquifer, is situated between the clay and basement layers, both of which have impermeable properties. . The identification of the existence of this aquifer layer is supported by data from residents' wells at the research location showing that there are drilled wells at a depth of \pm 40 m.

Based on the measurement results of sounding point 3 (**Figure 7**), the aquifer layer at point 3 is in the sand layer (fourth layer) which is interpreted as a confined aquifer because it is at a depth of 13.6 m – 61.8. It is interpreted as a confined aquifer because it is located quite deep and is limited by an aquiclude layer. Determining the confined aquifer layer is also based on the conditions for its existence, namely below the aquifer layer and above the aquifer layer which is impermeable, the third and fifth layers are impermeable layers. The identification of the existence of this aquifer layer is supported by data from residents' wells at the research location showing that there are shallow wells at a depth of \pm 5 m and drilled wells at a depth of \pm 40 m.

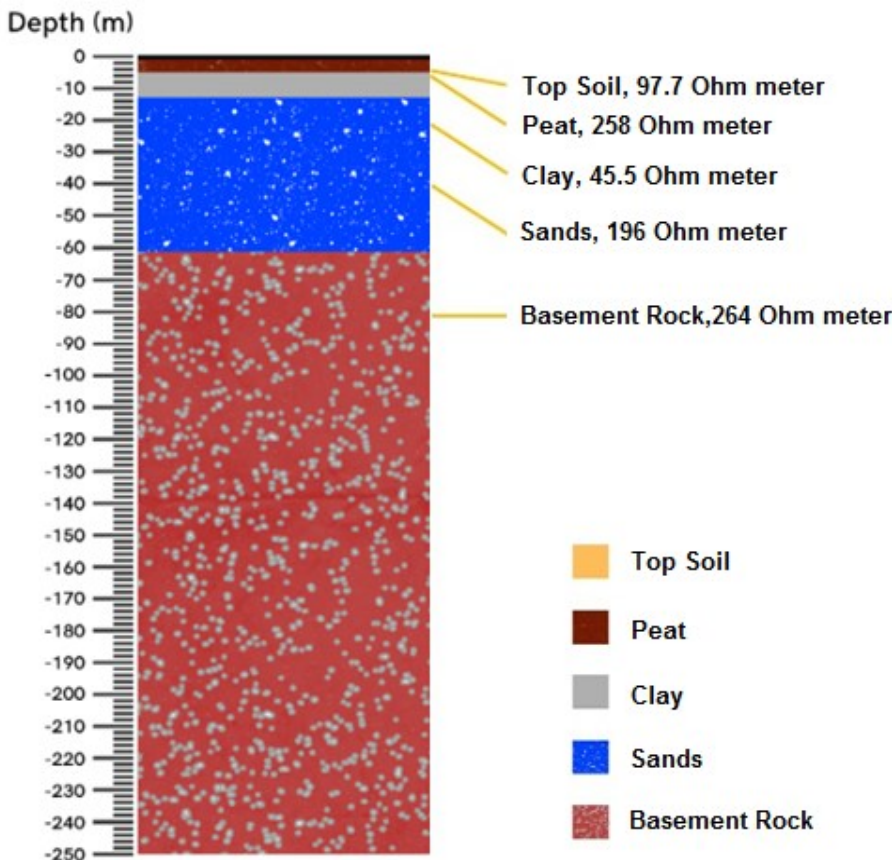


Figure 7. Lithology at sounding point 4

Table 2. Aquifer layers at the research location

VES point	Depth (m)	Thickness (m)	Lithology	Aquifer type
1	5,19 -35,5	30,3	Sand	Free
2	3,94 - 47,3	43,4	Sand	Free
3	25,8 - 44	18,2	Sand	Stressed
4	13,6 - 61,8	48,2	Sand	Stressed

Source : Data of this study

Based on the results of measurements from 4 sounding points at the research location, it can be found that the aquifer layer is unconfined aquifer and confined aquifer as in **Table 2**. The aquifer layer at the research location is interpreted as sand due to its large porosity and permeability properties, enabling it to accommodate and drain water, which are requirement for the aquifer layer. This layer is dominated by sand material which has quite large groundwater potential because it has quite high permeability and is porous, causing this layer to have quite large water flow and has the potential to store a lot of water and can function as an aquifer layer.

CONCLUSION

Based on the research results, the distribution of subsurface resistivity values obtained by sounding at the research location is $2.69 \Omega\text{m} - 264 \Omega\text{m}$, where after subsurface interpretation it is known that the type of rock that makes up the layer is the top soil layer which has a resistivity of $32 \Omega\text{m} - 98.8 \Omega\text{m}$, The peat layer has a resistivity value of $108 \Omega\text{m} - 258 \Omega\text{m}$, sand has a resistivity value of $2.69 \Omega\text{m} - 19.6 \Omega\text{m}$, clay has a resistivity value of $36.8 \Omega\text{m} - 45.5 \Omega\text{m}$, and bedrock has a resistivity value of $115 \Omega\text{m} - 264 \Omega\text{m}$. The research results show that the unconfined aquifer layer at point 1 and point 2 is at a depth of $3.94 \text{ m} - 35.5 \text{ m}$. Meanwhile, the depth of the confined aquifer layer at point 3 and point 4 is at a depth of $13.6 \text{ m} - 61.8 \text{ m}$.

ACKNOWLEDGMENT

The authors would like to thank all reviewers who have provided suggestions to improve this article.

CONFLICTS OF INTEREST

The authors declare no conflict of interest concerning the publication of this article. The authors also confirm that the data and the article are free of plagiarism.

REFERENCES

Abidin, H. Z., Andreas, H., Gumilar, I., Fukuda, Y., Pohan, Y. E., & Deguchi, T. (2011). Land subsidence of Jakarta (Indonesia) and its relation with urban development. *Natural Hazards*, 59(3), 1753–1771. <https://doi.org/10.1007/s11069-011-9866-9>

Aizebeokhai, A. P., & Oyeyemi, K. D. (2015). Application of geoelectrical resistivity imaging and VLF-EM for subsurface characterization in a sedimentary terrain, Southwestern Nigeria. *Arabian Journal of Geosciences*, 8(6), 4083–4099. <https://doi.org/10.1007/s12517-014-1482-z>

Al-ahmadi, M. E., & El-Fiky, A. A. (2009). Hydrogeochemical evaluation of shallow alluvial aquifer of Wadi Marwani, western Saudi Arabia. *Journal of King Saud University - Science*, 21(3), 179–190. <https://doi.org/10.1016/j.jksus.2009.10.005>

Anggereni, S., & Iqbal, M. S. (2018). Analysis of Physics Laboratory Management at The Northern Region of Makassar's State Senior High Schools By Standard of Facilities and Infrastructure. *Jurnal Ilmiah Pendidikan Fisika Al-Biruni*, 7(1), 41. <https://doi.org/10.24042/jipfalfbiruni.v7i1.2329>

Bott, L. M., Schöne, T., Illigner, J., Haghshenas Haghghi, M., Gisevius, K., & Braun, B. (2021). Land subsidence in Jakarta and Semarang Bay – The relationship between physical processes, risk perception, and household adaptation. *Ocean and Coastal Management*, 211. <https://doi.org/10.1016/j.ocecoaman.2021.105775>

Brindha, K., & Elango, L. (2012). Groundwater quality zonation in a shallow weathered rock aquifer using GIS. *Geo-Spatial Information Science*, 15(2), 95–104. <https://doi.org/10.1080/10095020.2012.714655>

Custodio, E. (2015). *Trends In Groundwater Pollution: Loss Of Groundwater Quality & Related Services*. Technical University of Catalonia.

FAO. (2016). Thematic Papers on Groundwater. In *Groundwater Governance – A Global Framework for Action*.

Fatchurohman, H., Adji, T. N., Haryono, E., & Wijayanti, P. (2018). Baseflow index assessment and master recession curve analysis for karst water management in Kakap Spring, Gunung Sewu. *IOP Conference Series: Earth and Environmental Science*, 148(1). <https://doi.org/10.1088/1755-1315/148/1/012029>

Gordon, B., Callan, P., & Vickers, C. (2008). WHO guidelines for drinking-water quality. *WHO Chronicle*, 38(3), 564. [https://doi.org/10.1016/S1462-0758\(00\)00006-6](https://doi.org/10.1016/S1462-0758(00)00006-6)

Handayani, P. M., & Puspasari, P. (2020). Learning From Palu: Rebuilding A Better City in The Aftermath of Natural Disaster. *Jurnal Pertahanan*, 6(3), 442–457.

Kamiya, T., & Hosono, H. (2010). Material characteristics and applications of transparent amorphous oxide semiconductors. *NPG Asia Materials*, 2(1), 15–22. <https://doi.org/10.1038/asiamat.2010.5>

Li, J., Zhou, Q., & Campos, L. C. (2018). The application of GAC sandwich slow sand filtration to remove pharmaceutical and personal care products. *Science of the Total Environment*, 635, 1182–1190. <https://doi.org/10.1016/j.scitotenv.2018.04.198>

Meijaard, E., Dennis, R. A., Saputra, B. K., Draugelis, G. J., Qadir, M. C. A., & Garnier, S. (2019). Rapid Environmental and Social Assessment of Geothermal Power Development in Conservation

Forest of Indonesia. *Proceedings World Geothermal Congress 2020 Reykjavik, Iceland, April 26 – May 2, 2020*, August, 1–12.

Négrel, P., Millot, R., Brenot, A., & Bertin, C. (2010). Lithium isotopes as tracers of groundwater circulation in a peat land. *Chemical Geology*, 276(1–2), 119–127. <https://doi.org/10.1016/j.chemgeo.2010.06.008>

Nomura, K., Ohta, H., Takagi, A., Kamiya, T., Hirano, M., & Hosono, H. (2004). Room-temperature fabrication of transparent flexible thin-film transistors using amorphous oxide semiconductors. *Nature*, 432(7016), 488–492. <https://doi.org/10.1038/nature03090>

Poirrasson, F., Dundas, S. H., Toutain, J. P., Munoz, M., & Rigo, A. (1999). Earthquake-related elemental and isotopic lead anomaly in a springwater. *Earth and Planetary Science Letters*, 169(3–4), 269–276. [https://doi.org/10.1016/S0012-821X\(99\)00085-0](https://doi.org/10.1016/S0012-821X(99)00085-0)

Prabowo, A., Hartono, H., & Kaeni, O. (2022). Analisis Potensi Air Tanah Menggunakan Metode Vertical Electrical Sounding (Ves) Di Kelurahan Hargomulyo. *JGE (Jurnal Geofisika Eksplorasi)*, 8(2), 81–92. <https://doi.org/10.23960/jge.v8i2.189>

Pratiwi, E. S., Sartohadi, J., & Wahyudi. (2019). Geoelectrical Prediction for Sliding Plane Layers of Rotational Landslide at the Volcanic Transitional Landscapes in Indonesia. *IOP Conference Series: Earth and Environmental Science*, 286(1). <https://doi.org/10.1088/1755-1315/286/1/012028>

Sabara, Z., Anwar, A., Yani, S., Prianto, K., Junaidi, R., Umam, R., & Prastowo, R. (2022). Activated Carbon and Coconut Coir with the Incorporation of ABR System as Greywater Filter: The Implications for Wastewater Treatment. *Sustainability (Switzerland)*, 14(2), 1026. <https://doi.org/https://doi.org/10.3390/su14021026>

Sadjab, B. A., Indrayana, I. P. T., Iwamony, S., & Umam, R. (2020). Investigation of The Distribution and Fe Content of Iron Sand at Wari Ino Beach Tobelo Using Resistivity Method with Werner-Schlumberger Configuration. *Jurnal Ilmiah Pendidikan Fisika Al-Biruni*, 9(1), 141–160. <https://doi.org/10.24042/jipfalfbiruni.v9i1.5394>

Saparun, M., Akbar, R., Marbun, M., Dixit, A., & Saxena, A. (2022). *Application of Induced Polarization and Resistivity to the Determination of the Location of Minerals in Extrusive Rock Area, Southern Mountains of Java, Indonesia*. 1(3), 108–119.

Satriani, A., Loperte, A., Imbrenda, V., & Lapenna, V. (2012). Geoelectrical surveys for characterization of the coastal saltwater intrusion in metapontum forest reserve (Southern Italy). *International Journal of Geophysics*, 2012. <https://doi.org/10.1155/2012/238478>

Savira, F., & Suharsono, Y. (2013). Information on Conductivity Measurement. *Journal of Chemical Information and Modeling*, 01(01), 1689–1699.

Sudirman, Trisutomo, S., Barkey, R. A., & Ali, M. (2018). Watershed Identification and Its Effect Toward Flood (Case Study: Makassar City). *International Journal of Advanced Research*, 6(5), 513–519. <https://doi.org/10.21474/ijar01/7059>

Team, A. D. (2016). *Country Water assessment Indonesia Country Water assessment*. www.adb.org

Tsunomori, F., Shimodate, T., Ide, T., & Tanaka, H. (2017). Radon concentration distributions in shallow and deep groundwater around the Tachikawa fault zone. *Journal of Environmental Radioactivity*, 172, 106–112. <https://doi.org/10.1016/j.jenvrad.2017.03.009>

You, C. F., Castillo, P. R., Gieskes, J. M., Chan, L. H., & Spivack, A. J. (1996). Trace element behavior in hydrothermal experiments: Implications for fluid processes at shallow depths in subduction zones. *Earth and Planetary Science Letters*, 140(1–4), 41–52. [https://doi.org/10.1016/0012-821X\(96\)00049-0](https://doi.org/10.1016/0012-821X(96)00049-0)

Zoysa, R. S. De, Schöne, T., Herbeck, J., Illigner, J., Haghghi, M., Simarmata, H., Porio, E., Rovere, A., & Hornidge, A. K. (2021). The “wickedness” of governing land subsidence: Policy perspectives from urban southeast Asia. *PLoS ONE*, 16(6 (June)), 1–25. <https://doi.org/10.1371/journal.pone.0250208>